2013 International Conference on Advances in ICT for Emerging Regions (ICTer): 015 - 020

Active Contour-based Segmentation and Removal of Optic Disk from Retinal Images

M.H.S.P. Kumara and R.G.N. Meegama

Department of Statistics and Computer Science, Faculty of Applied Sciences
University of Sri Jayewardenepura
Gangodawila, Nugegoda, Sri Lanka
rgn@sci.sjp.ac.lk

***Abstract*—A retinal fundus photograph is widely used in the diagnosis and treatment of various eye diseases such as diabetic retinopathy and glaucoma. Computer-aided analysis of fundus images provides an immediate detection and characterization of retinal features prior to inspection by a specialist. Segmentation of structures in such a retinal image can be used to detect and calculate the geometric shape and size of the optic disc and anterior segment with abnormal growth of any region in the eye. In this paper, we propose an algorithm based on active contours, often referred to as snakes, to remove the optic disk from retinal images. The proposed method consists of two main steps. In the first step, the optic disk boundary is approximated by means of edge detection, morphological operations and circular Hough transformation. In the second step, the exact boundary of the optic disk boundary is detected using an active contour model. The proposed algorithm was tested using 130 colored fundus images. Among those images, 20 were normal and 110 contained signs of the diabetic retinopathy. Results indicate a 90% accuracy in detecting the optic disc by the proposed technique.**

***Keywords*— Active contours, optic disc, retinal images**

I. INTRODUCTION

The eye is one of the most sensitive organs of the human body. There are many diseases that can affect the eye including those diseases that can damage the optical disk. These diseases result in several types of retinopathy in the retina such as diabetic retinopathy, non-proliferative diabetic retinopathy, proliferative diabetic retinopathy, hypertensive retinopathy, arteriosclerotic retinopathy and retinopathy of prematurity.

To identify such retinopathy, we obtain an image of the eye often referred to as a retinal image. Such retinal images are obtained using a fundus camera which is specifically designed for this purpose. This camera can take a perfect image by creating a photograph of the interior surface of the eye including the retina, optic disk, macula, and posterior pole.

The retina is a light-sensitive tissue lining the inner surface of the eye. The optics of the eye creates an image of the visual world on the retina. Light rays that fall on the retina trigger chemical and electrical events activating nerve impulses to the brain. The optic disk is located on the retina of the eye and is referred to as the physiological blind spot of the eye. The disc is the location where ganglion cell axons leave the eye forming the optic nerve. At this spot, there are no light sensitive photoreceptor cells to respond to a light stimulus.

Whenever an eye is subjected to retinopathy, it is very difficult to separately identify the disease that affects the optical disk. This paper proposes a technique based on active contours to detect and separate the optical disk from other structures of the eye so that diagnosis of any disease of the eye is possible at an early stage.

Detection and treatment of diabetic retinopathy at an early stage is vital because ophthalmologist would then be able to treat the patients by advanced laser treatment before serious complications, such as total blindness, would occur.

II. RECENT WORK

Mendels et al. [1] have proposed a technique based on active contour driven external forces where the original image is pre-processed to minimize incorrect boundary detection due to blood vessels crossing the optic disk. The pre-processing step is based on local minima detection and morphological filtering. After pre-processing, the optic disk boundary is determined using an external image-derived field called the Gradient Vector Flow (GVF). This technique, however, does not indicate that the initial contour of the snake is determined automatically and moreover, the method was tested with only 9 images. Also, a quantitative measurement for the accuracy in detecting the optic disc is not provided in the paper.

A method based on principal component analysis is employed to locate the optic disk in [2] where a modified active shape model (ASM) is proposed to detect the optic disk. A fundus coordinate system is defined to support an improved description of features of interest in retinal images. The success rate of detecting the boundary of the optic disk is reported to be 94% where such success rates of this algorithm could be attributed to the utilization of model-based methods.

Xu et al. [2] have presented a deformable-model based approach to detect the optic disk and cup boundaries in retinal images. This method has improved and extended the original snake model in two aspects: knowledge-based clustering and smoothing update. The snake deforms while minimizing the

978-1-4799-1276-6/13/$31.00 ©2013 IEEE

energy and then self-clusters into two groups, i.e., an edge-point group and an uncertain-point group, which are determined by a combination of both local and global information. These modifications provide the required flexibility to the contour to become more accurate and robust to occlude blood vessels, noise, poorly contrasted edges and fuzzy contour shapes. The experiments performed on 100 images indicate the success rate of the technique as 94%, when compared to those obtained by GVF-snakes as 12% and modified ASM as 82%.

The above techniques presented in literature suffer from the drawback that the contour needs to be manually initialized by the user, thus, cannot be used to automatically extract the optic disk from images in a large database.

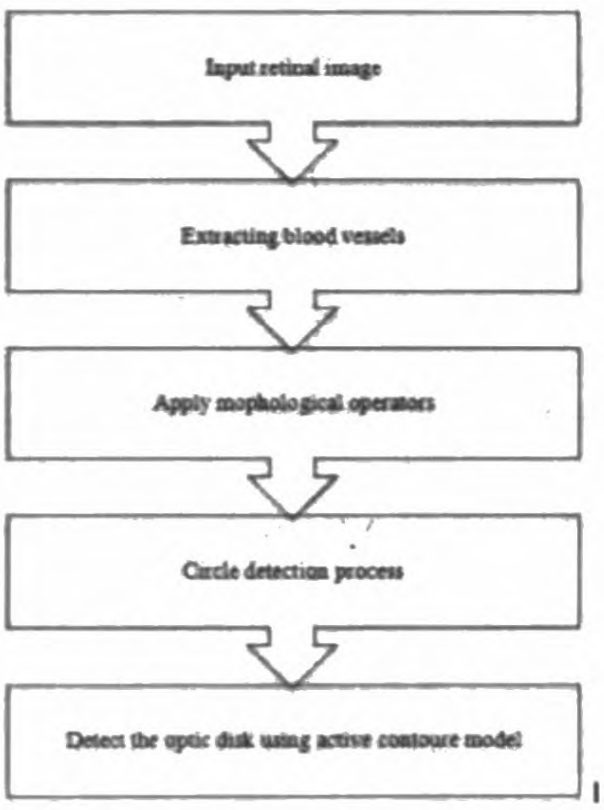

Figure 1. Main stages of the proposed algorithm

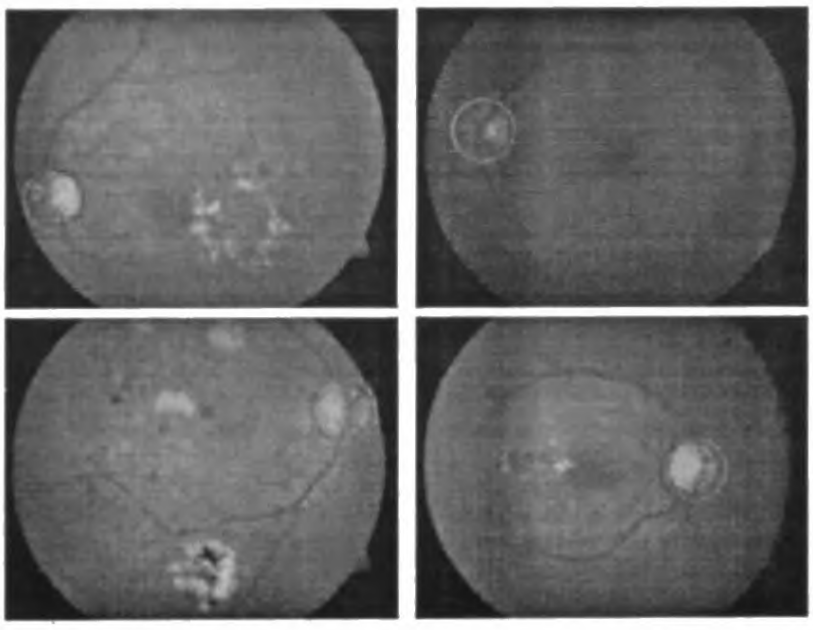

Figure 2. Location of optic disk in retinal images: (top row) left side and (bottom row) right side.

III. PROPOSED METHODOLOGY

The algorithm proposed in this paper detects and removes the optic disc using principles of mathematical morphology and active contours in a pipeline of routines as shown in Figure 1. At the initial stage, the boundary of the optic disc is approximated using mathematical morphology. This stage can be divided into several sub-stages, namely, pre-processing, extraction of blood vessels and approximate detection of the optic disc. Pre-processing involves noise removal using Gaussian filtering [3].

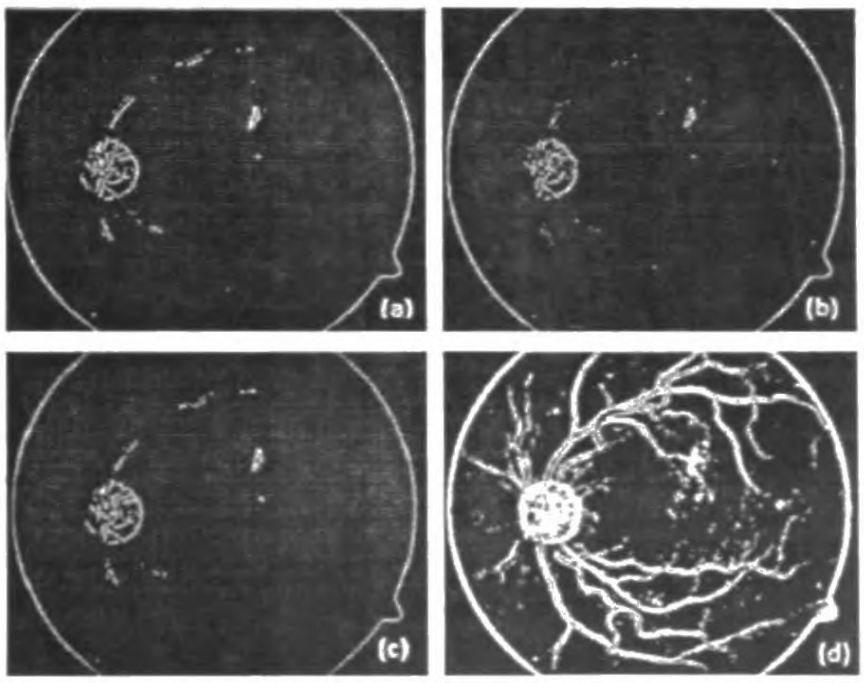

Figure 3. Detection of edges using (a) Sobel, (b) Roberts, (c) Prewitt and (d) Kirsch operator.

The process for the approximation of the optic disk boundary is the second process out of the stated four main processes. Approximation of the optic disk is essential prior to actual detection of the boundary because the optic disk does not always exist in the same position within retinal images as seen in Figure 2. As such, it is apparent that the optic disk can be anywhere within a retinal image since it has no exact position within the retina.

After removal of noise, the blood vessels and the approximate location of the optic disk need to be extracted using an edge detection algorithm. Among several edge detection algorithms [4, 5] we selected the Kirsch operator. The selection of the Kirsch operator is due to several reasons. First and foremost, the optic disk has a circular shape. This means, edges are present in all directions and as such, the edge detection method must be capable of extracting such edges in each and every direction. We can achieve the desired results by using the Kirsch operator as seen in Figure 3 where four output images were obtained by applying four widely used edge detection algorithms as mentioned above. The Kirsch operator extracts both blood vessels and the optic disk in retinal images. As such, these blood vessels need to be removed in order to isolate and segment only the optic disk. This process mainly consists of three sub processes, namely, application of median filter, filling of holes and morphological opening. The output images obtained after each of these sub processes are depicted in Figure 4.

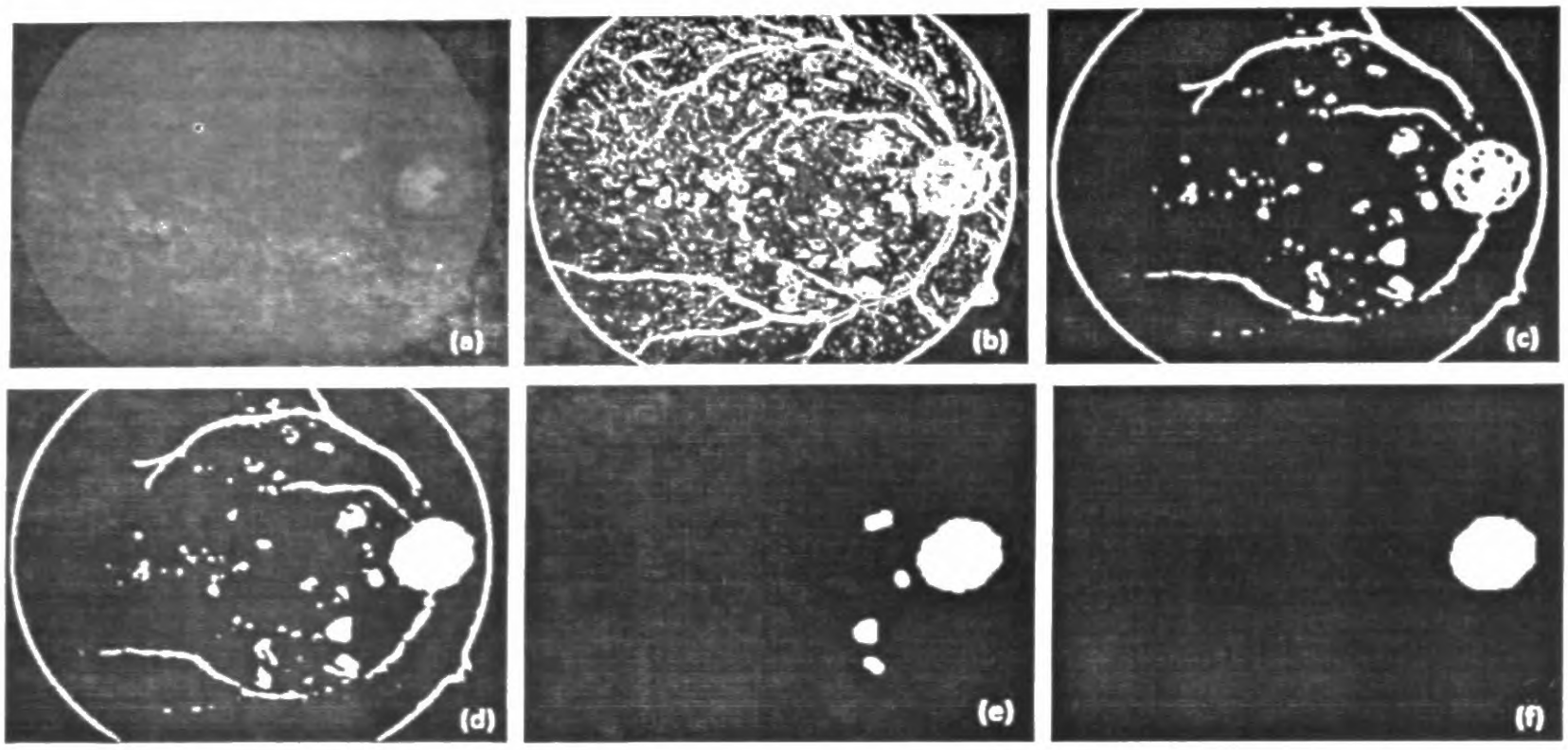

Figure 4. Output images of detection of approximate optic disc: (a) original image, (b) applying Kirch operator (c) median filtering, (d) filling of holes, (e) morphological opening with structuring element having radius 5 and (f) morphological opening with a structuring element having radius 10.

The median filter is specifically used at this stage as it preserves edges while removing noise. In this application, it removes noise within the image without having any adverse effects on the shape of the boundary of the optic disk.

As the edge detection algorithm has removed some wanted regions inside the optic disk, a hole filing routine is applied on the median filtered image to recover these regions. Subsequently, a morphological opening procedure is applied to remove blood vessels that can be seen as narrow paths spreading out from the optic disk area.

A. Approximate detection of optic disk boundary

The main purpose of this process is to obtain an initial set of points surrounding the extracted optic disk. These points are later to be used as initial control points for the active contour (often referred to as snakes). This task is achieved using the Hough transformation [6] that attempts to find imperfect instances of objects within a certain class of shapes by a voting procedure.

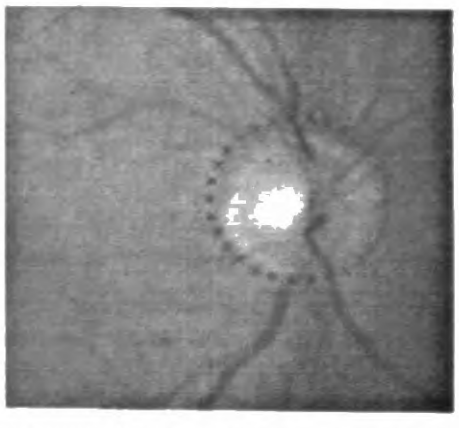

Figure 5. Approximate contour surrounding the optic

Figure 5 illustrates the approximated optic disk boundary obtained using the Hough transformation. Approximation of the boundary of the optic disk was carried out on the images available in the database while empirically changing the threshold value as given in TABLE 1. As seen, when value of the threshold is increased, the accuracy of the approximation decreases.

TABLE 1.
Accuracy of approximate detection of the boundary of optic disk (out of 130 images)

Threshold value	Number of images with correct boundary	Percentage (%)
3	117	90.0
7	103	79.23
10	87	66.9

Moreover, the shape of the structuring element used for morphological opening described in the previous step affects the accuracy of detecting the approximate boundary of the optic disk. The numbers of images consisting of accurate approximate boundary of the optic disk (out of 130 images) are given in TABLE 2.

For this experiment, a diamond structuring element (having a distance = 3), a disk (having a radius = 3), and a line (having a length = 5, angle = 45 degrees) were used. As seen, the diamond shaped structuring element resulted in extracting the approximate boundary with a higher accuracy than using other structuring elements.

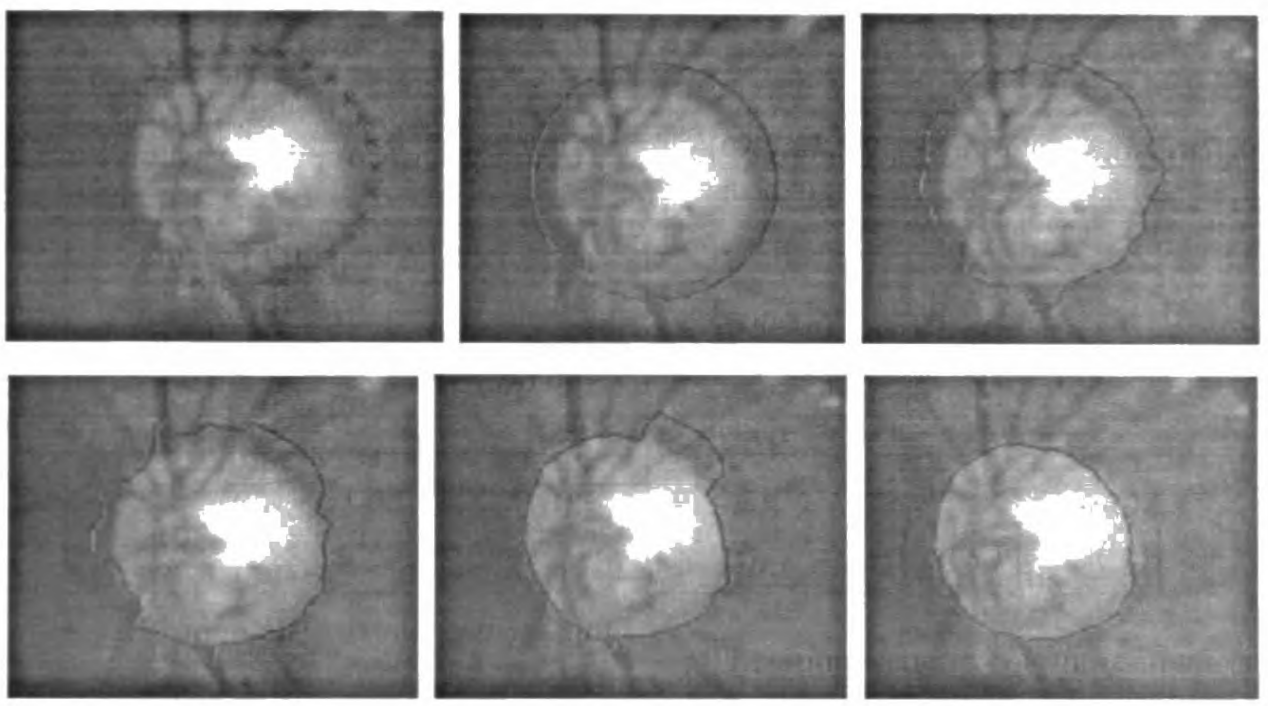

Figure 6. Output images of active contour segmentation of optic disc: (a) initial contour points, (b) initial contour, (c) contour after 50 iterations, (d) contour after 100 iterations, (e) contour after 200 iterations and (f) contour after 500 iterations.

TABLE 2. Accuracy of approximate detection of the boundary of optic disk based on the shape of the structuring element (out of 130 images).

Shape of structuring element	Number of images with correct boundary	Percentage (%)
diamond (distance 3)	117	90.00
disk (radius 3)	106	81.50
line (45° angle, length 5)	98	75.38

B. Detection of optic disk boundary using active contour method

Up to this point, a set of points that surrounds the optic disk has been detected approximately and the initial contour, prepared using these points, needs to be fit into the actual boundary of the optic disk. Active contour models have been widely used in medical image segmentation in recent times [8 – 10]. The mathematical framework of the Active contour is given as follows:

A retinal grey-scale image I is defined in the $x-y$ image plane, with $I(x,y)$ denoting the value of luminance at position (x,y). An active contour is defined as a parametric curve $v(s) = [x(s)\, y(s)]$ in the plane, with s as a normalised parameter representing a position on the curve; $s \in [0,1]$ and $v(s)$ depends on time [7].

The total energy of an active contour, E_{snake}, defined as,

$$E_{Snake} = \int_0^1 E_{Snake}\,(v(s))ds \qquad (1)$$

If E_{int} and E_{ext} represent the internal and external energy of the snake, respectively, E_{snake} can be written as:

$$\boldsymbol{E_{Snake} = \int_0^1 E_{Int}(v(s)) + E_{Ext}(v(s))\, ds} \qquad (2)$$

where

$$E_{Int} = \frac{1}{2}\left(\alpha(s)\left|\frac{d}{ds}v(s)\right|^2 + \beta(s)\left|\frac{d^2}{ds^2}v(s)\right|^2\right) \qquad (3)$$

The spline energy of the contour is composed of first and second order terms where the first order term is governed by by $\alpha(s)$ adjusting the elasticity (tension) of the snake whereas the second order term is controlled by $\beta(s)$ adjusting the stiffness (rigidity) of the snake. The first order term makes the snake act like a membrane while second order term makes it act like a thin plate.

The external energy of the active contour is represented as:

$$E_{ext} = w_{line}E_{line} + w_{edge}E_{edge} \qquad (4)$$

where,
$E_{line} = I(x,y)$, $E_{edge} = -|\nabla I(x,y)|^2$,
w_{line} = weighing factor for intensity based potential term,
w_{edge} = weighing factor for edge based potential term and ∇ denotes the gradient operator. Minimizing the energy functional of equation 2 results in the following independent Euler equation:

$$\alpha\left(\frac{\partial^2 v}{\partial x^2}\right)+\beta\left(\frac{\partial^4 v}{\partial x^4}\right)+(\nabla E_{ext})=0 \quad (5)$$

$$\alpha\begin{pmatrix}\frac{\partial^2 v}{\partial x^2}\\ \frac{\partial^2 v}{\partial y^2}\end{pmatrix}+\beta\begin{pmatrix}\frac{\partial^4 v}{\partial x^4}\\ \frac{\partial^4 v}{\partial y^4}\end{pmatrix}+\begin{pmatrix}\frac{\partial E_{ext}}{\partial x}\\ \frac{\partial E_{ext}}{\partial y}\end{pmatrix}=\begin{pmatrix}0\\0\end{pmatrix} \quad (6)$$

In order to approximate the derivatives with finite differences, we first define a set of N nodes v_i for the active contour as:

$$v_i=\begin{pmatrix}x_i\\ y_i\end{pmatrix}=\begin{pmatrix}x[ih]\\ y[ih]\end{pmatrix} \quad (7)$$

with $i=0,1,2,\ldots\ldots,N-1, h=1/N$. The discretization step for s, $E_{Int}(i)$ can be expanded as:

$$E_{Int}(i)=\frac{\alpha_i|v_i-v_{i-1}|^2}{2h^2}+\frac{\beta_i|v_{i-1}-2v_i+v_{i+1}|^2}{2h^4} \quad (8)$$

where $v_0=v_N$.

Let $f_x(i)=\partial E_{Ext}/\partial x$ and $f_y(i)=\partial E_{Ext}/\partial y$ where the derivatives are approximated by a finite difference if they cannot be computed analytically. Now, the corresponding Euler equation can be written as:

$$\alpha_i(v_i-v_{i-1})-\alpha_{i+1}(v_{i+1}-v_i)+\beta_{i-1}(v_{i-2}-2v_{i-1}+v_i)$$
$$-2\beta_i(v_{i-1}-2v_i+v_{i+1})+\beta_{i+1}(v_i-2v_{i+1}+v_{i+2})+$$
$$\left(f_x(i),f_y(i)\right)=0 \quad (9)$$

The above Euler equation can also be expressed as:

$$\boldsymbol{A}\begin{pmatrix}\boldsymbol{x}\\ \boldsymbol{y}\end{pmatrix}+\begin{pmatrix}\boldsymbol{f_x}\\ \boldsymbol{f_y}\end{pmatrix}=\boldsymbol{0} \quad (10)$$

where, A is a penta-diagonal banded matrix. To solve equation 10, we set the right hand side of the equation equal to the product of a step size and the negative time derivatives of the left hand sides. Taking into account derivatives of the external forces requires changing A at each iteration. We can achieve fast iteration by assuming that f_x and f_y remain constant at each time step yielding an explicit Euler method with respect to external forces of the snake. Because internal forces are all defined by the banded matrix we only need to evaluate the time derivative at time t (iteration t) rather than at time $t-1$ (iteration$t-1$).

The resulting equation is given as:

$$A\begin{pmatrix}x_t\\ y_t\end{pmatrix}+\begin{pmatrix}f_x(x_{t-1},y_{t-1})\\ f_y(x_{t-1},y_{t-1})\end{pmatrix}=\begin{pmatrix}-\gamma(x_t,x_{t-1})\\ -\gamma(y_t,y_{t-1})\end{pmatrix}$$

where γ is a step size. When convergence is achieved (minimized energy state), the time derivative vanishes and this iteration ends up with a solution to equation 10.

Removal of optic disk process

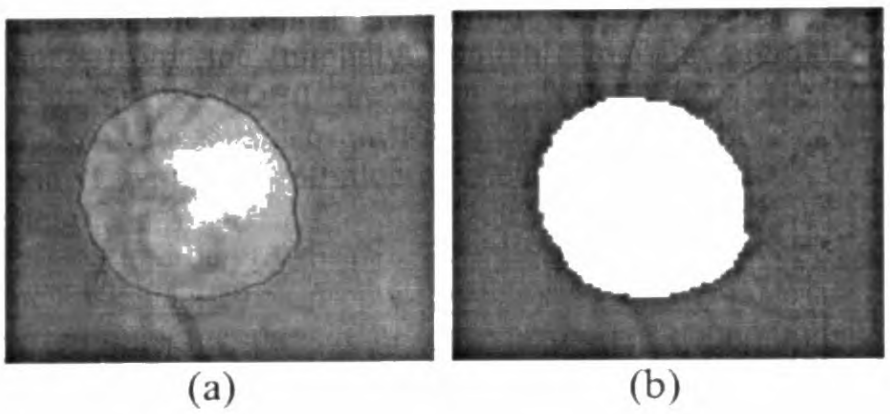

(a) (b)

Figure 7. Removal of optic disc (a) active contour converged on optic disc and (b) optic disc removed.

Figure 7 depicts the actual optic disc boundary obtained by the active contour and subsequently the disk removed from the retinal image.

IV. RESULTS AND DISCUSSION

For testing the proposed algorithm, we have chosen forty images from the publicly available diabetic retinopathy dataset DIARETDB0 and DIARETDB1 [12, 13]. These images were taken from Kuopio University hospital and captured with few 50 degree field-of-view digital fundus cameras.

In order to measure the accuracy in extracting the optic disk using the proposed technique, we used a metric referred to as the average distance error. The actual boundary of an optic disc within a current fundus image is manually traced using a free hand tool. If this manually traced boundary (ground truth) is taken as $\hat{v}(s)$ and the boundary extracted from the proposed active contour process is taken as $v(s)$, the average distance error e is defined as:

$$e\left(\hat{v}(s),v(s)\right)=\frac{1}{n_p}\int_0^1 \min\left(\hat{v}(s)-v(s)\right)ds$$

where n_p gives the number of pixels within$v(s)$..

The distance errors obtained after extracting the optic disk from the images in the database are given in TABLE 3. It is apparent that the optic disk was extracted with an average distance error of at most 0.5 in more than 45% of the images.

TABLE 3.
Number of images with average distance errors.

Number of images (out of 130)	Average distance error is less than (<)	Percentage (%)
15	0.1	11.54
5	0.2	03.85
15	0.3	11.54
16	0.4	12.31
15	0.5	11.54
6	0.6	04.62
12	0.7	09.23
8	0.8	06.15
11	0.9	08.46
11	1.0	08.46

Images having large distance errors are given in TABLE 34. Such large values for this metric are primarily due to improper removal of blood vessels during morphological processing. In these instances, the optic disk is cannot be approximated accurately properly and as such, the active contour may wiggle out of the required boundary. The methodology needs to be improved to automatically remove blood vessels in the images without user intervention.

TABLE 4.
Images having large average distance errors.

Image	Average distance error
image019.png	131.61
image020.png	150.618
image029.png	15.9427
image042.png	49.0499
image046.png	5.15437
image048.png	62.8687
image057.png	8.14882
image061.png	140.999
image067.png	65.3113
image093.png	36.2276
image097.png	2.11073
image098.png	16.1514
Image112.png	12.5063

V. CONCLUSION

In this research, a computer aided retinal image analysis system for the segment of optic disk in color digital fundus images using active contours is presented. The active contour is initiated by pre-processing the fundus image where the boundary of the optic disk is first approximated automatically. This approximation enables placement of initial points of the active contour surrounding the optic disk. Such a mechanism is useful in applications where large number of retinal images in a database need to be processed to remove the optic disk because the automated approximation of the optic disk avoids manual placement of initial control points of the active contour.

The proposed algorithm was tested for retinal images containing both soft and hard exudates. It is prudent to test the algorithm with several image databases before the technique is applied for clinical use.

REFERENCES

[1] F. Mendels, C. Heneghan and J. Thiran, Identification of the optic disk boundary in retinal images using active contours, Proceedings of Irish Machine Vision and Image Processing Conference, pp. 103–115, 1999.

[2] J. Xua, O. Chutatapeb, E. Sungc, C. Zhengd and P. C. T. Kuand, Optic disk feature extraction via modified deformable model technique for glaucoma analysis, Pattern recognition 40.7 (2007): 2063-2076.

[3] Gaussian blur, [Online]. Available: http://en.wikipedia.org/wiki/Gaussian_blur.

[4] T.-H. H. Lee, Edge Detection Analysis. Graduate institute of communication engineering, Taipei, Taiwan, ROC (2007)

[5] R. Maini and D. H. Aggarwal, Study and Comparison of Various Image Edge Detection Techniques, International Journal of Image Processing, vol. 3, no. 1, 2009.

[6] S. Sekhar, W. Al-Nuaimy and A. K. Nandi, Automated Localization of Retinal Optic Disk Using Hough Transform, IEEE Int. Symp. Biomedical Imaging: From Nano to Macro, 2008.

[7] M. Kass, A. Witkin and D. Terzopoulos, Snakes: Active Contour Models, International Journal of Computer Vision, vol. 1, no. 4, pp. 321-331, 1988.

[8] G. Aubert, M. Barlaud, O. Faugeras and S. Jehan-Besson, Image segmentation using active contours: calculus of variations or shape gradients?, SIAM Journal on Applied Mathematics, vol. 63, no. 6, pp. 2128-2154, 2002.

[9] Pham, Dzung L., Chenyang Xu, and Jerry L. Prince. "Current methods in medical image segmentation 1." Annual review of biomedical engineering 2.1 (2000): 315-337.

[10] S. Weeratunga and C. Kamath, An Investigation of Implicit Active Contours for Scientific Image Segmentation, Proceedings of SPIE, vol. 5308, pp. 210-221. 2004.

[11] Region of Interest, [Online]. Available: http://en.wikipedia.org/wiki/Region_of_Interest.

[12] Standard Diabetic Retinopathy Database, IMAGERET, [Online]. Available: http://www2.it.lut.fi/project/imageret/diaretdb0/.

[13] T. Kauppi, V. Kalesnykiene, J-K. Kamarainen, L. Lensu and I. Sor, DIARETDB0: Evaluation Database and Methodology for Diabetic Retinopathy Algorithms, Technical report, 2006.